Inorg. Chem. **2005**, *44*, 6736–6743

Calix[4]pyrrole Schiff Base Macrocycles: Novel Binucleating Ligands for Cu(I) and Cu(II)

Jacqueline M. Veauthier,[†] Elisa Tomat,[†] Vincent M. Lynch,[†] Jonathan L. Sessler,*[,†] Utkir Mirsaidov,[‡] and John T. Markert*[,‡]

Department of Chemistry and Biochemistry, 1 University Station A5300, The University of Texas at Austin, Austin, Texas 78712-0165, and Department of Physics, 1 University Station C1600, The University of Texas at Austin, Austin, Texas 78712-0264

Received May 3, 2005

New bimetallic copper(I) and copper(II) complexes of dipyrromethane-derived Schiff base macrocycles are reported. Two different structural motifs were identified, providing support for the notion that ligands of this type can support a variety of coordination modes. In the case of the Cu(I) complexes, the metal centers were found to have a distorted tetrahedral geometry and be coordinated to two imine nitrogens on each side of the ligand, with the exact structure depending on the choice of Schiff base macrocycle. In contrast to what is seen for Cu(I), with Cu(II) as the coordinated cation the Cu(II) metal centers assumed distorted square planar geometries, and both pyrrole N–Cu and imine N–Cu interactions were confirmed by single-crystal X-ray diffraction analysis. This structural analysis revealed a copper–copper distance of 3.47 Å, while SQUID magnetic susceptibility data provided evidence for antiferromagnetic coupling between the two metal centers.

Introduction

It is well known that the active sites of many enzymes are binuclear and contain coordinatively unsaturated metal ions held in close proximity (ca. 2.5−6.0 Å) within a flexible cavity. It is also known that the metal centers in these enzymes are often held in place by heterocyclic nitrogen-rich ligands, including those with imine functionality. While in biology the most common sources of imine-type nitrogen-donor ligands are imidazoles from histidine and pyrroles, within, e.g., heme, this kind of functionality is also a defining feature of expanded porphyrins. Expanded porphyrins, as the name implies, are a class of synthetic oligopyrrolic macrocycles that possess larger internal cavities than those present in naturally occurring tetrapyrroles. Many expanded porphyrins also contain a greater number of central donor atoms. This makes such systems of interest for the construction of multinuclear complexes that might act as models for the active sites of metalloenzymes. However, at present the number of well-characterized bimetallic complexes derived from oligopyrrolic macrocycles[1−15] remains rather limited, and it is likely that further studies of their fundamental coordination chemistry will be required before their potential

* E-mail: sessler@mail.utexas.edu.
[†] Department of Chemistry.
[‡] Department of Physics.

(1) Sessler, J. L.; Tomat, E.; Mody, T. D.; Lynch, V. M.; Veauthier, J. M.; Mirsaidov, U.; Markert, J. T. *Inorg. Chem.* **2005**, *44*, 2125−2127.
(2) Callaway, W. B.; Veauthier, J. M.; Sessler, J. L. *J. Porphyrin Phthalocyanine* **2004**.
(3) Veauthier, J. M.; Cho, W.-S.; Lynch, V. M.; Sessler, J. L. *Inorg. Chem.* **2004**, *43*, 1220−1228.
(4) Acholla, F. V.; Takusgawa, F.; Mertes, K. B. *J. Am. Chem. Soc.* **1985**, *107*, 6902−6908.
(5) (a) Reiter, W. A.; Gerges, A.; Lee, S.; Deffo, T.; Clifford, T.; Danby, A.; Bowman-James, K. *Coord. Chem. Rev.* **1998**, *174*, 343−359. (b) Gerasimchuk, N. N.; Gerges, A.; Clifford, T.; Danby, A.; Bowman-James, K. *Inorg. Chem.* **1999**, *38*, 5633−5636.
(6) Rongqing, L.; Mulder, T. A.; Beckmann, U.; Boyd, P. D. W.; Brooker, S. *Inorg. Chim. Acta* **2004**, 3360−3368.
(7) (a) Hannah, S.; Seidel, D.; Sessler, J. L.; Lynch, V. M. *Inorg. Chim. Acta* **2001**, *317*, 211−217. (b) Sessler, J. L.; Weghorn, S. J.; Hiseada, Y.; Lynch, V. M. *Chem. Eur. J.* **1995**, *1*, 56−67. (c) Sessler, J. L.; Gebauer, A.; Guba, A.; Scherer, M.; Lynch, V. M. *Inorg. Chem.* **1998**, *37*, 2073−2076. (d) Weghorn, S. J.; Sessler, J. L.; Lynch, V.; Baumann, T. F.; Sibert, J. W. *Inorg. Chem.* **1996**, *35*, 1089−1090.
(8) Xie, L. Y.; Dolphin, D. *J. Chem. Soc., Chem. Commun.* **1994**, 1475−1476.
(9) Adams, H.; Elsegood, M. R. J.; Fenton, D. E.; Heath, S. L.; Ryan, S. J. *J. Chem. Soc., Dalton Trans.* **1999**, 2031−2037.
(10) Rodríguez-Morgade, M. S.; Cabezón, B.; Esperanza, S.; Torres, T. *Chem. Eur. J.* **2001**, *7*, 2407−2413.
(11) Narayanan, S. J.; Sridevi, B.; Chandrashekar, T.; Englich, U.; Ruhland-Senge, K. *Inorg. Chem.* **2001**, *40*, 1637−1645.
(12) (a) Wytko, J. A.; Michels, M.; Zander, L.; Lex, J.; Schmickler, H.; Vogel, E. *J. Org. Chem.* **2000**, *65*, 8709−8714. (b) Bley-Escrich, J.; Gisselbrecht, J.-P.; Vogel, E.; Gross, M. *Eur. J. Inorg. Chem.* **2002**, 2829−2837.
(13) Givaja, G.; Blake, A. J.; Wilson, C.; Schroder, M.; Love J. B. *Chem. Commun.* **2003**, 2508−2509.

10.1021/ic050690d CCC: $30.25
Published on Web 08/09/2005

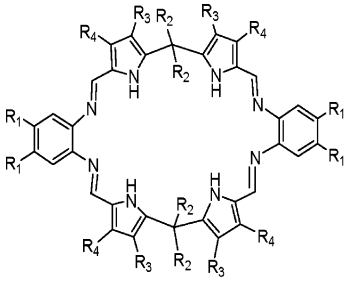

1 R_1 = H, R_2= CH_3, R_3= H, R_4= H
2 R_1 = OCH_3, R_2= CH_3, R_3= H, R_4= H
3 R_1 = H, R_2 = H, R_3 = CH_2CH_3, R_4= H

Figure 1. Calix[4]pyrrole Schiff base macrocycles.

use as putative enzyme mimics can be realized. With such considerations in mind, we recently prepared a class of new Schiff base calixpyrrole analogues (e.g., macrocycles **1** and **2**, see Figure 1) and showed that they were able to stabilize two different bimetallic μ-oxo-bridged iron complexes depending on the protonation state of the starting macrocycle.[3] This same ligand system has been independently prepared and studied by Love and colleagues,[13,16] who were able to demonstrate its utility in stabilizing a bis-Pd(II) and a mono-uranyl complex. In this paper we report the synthesis and characterization of bimetallic copper(I) complexes of macrocycles **1** and **2** and the corresponding copper(II) complex of **1**. In the latter complex magnetic susceptibility measurements indicate antiferromagnetic coupling between the two Cu(II) metal centers.

Experimental Section

General Procedures. All reactions and manipulations were carried out under an atmosphere of dry, oxygen-free argon by means of standard Schlenk techniques or a Vacuum Atmospheres drybox unless otherwise stated. Prior to use, all glassware were soaked in KOH-saturated isopropyl alcohol for ca. 12 h and then rinsed with water and acetone before being thoroughly dried. Air-sensitive filtrations were performed using positive argon pressure to force solutions through a specially constructed filtration cannula. The latter was made by fitting the port end of a stainless steel cannula with a piece of hardened filter paper (Whatman's No. 5) and then securing it with Teflon tape. The port of the cannula was made by welding a stainless steel filter support to one end of the cannula purchased from Popper & Sons Inc. Solutions were stirred magnetically.

Tetrahydrofuran (THF) was dried by passage through two columns of activated alumina. Dichloromethane was freshly distilled from calcium hydride. *n*-Pentane was stirred over concentrated H_2SO_4 for more than 24 h, neutralized with K_2CO_3, and distilled from CaH_2. Hexanes were purchased from Fisher Scientific and used as received. All deuterated NMR solvents were purchased from Cambridge Isotope Labs and used as received.

Unless otherwise stated, all reagents were used as received. Copper(I) mesitylene (Cu_5Mes_5)[17] and Schiff base macrocycles **1**[18] and **2**[18] were prepared according to previously published procedures.

Nuclear magnetic resonance (NMR) spectra were obtained on a Varian Mercury 400 MHz or a Brüker AC 250 MHz spectrometer. Low- and high-resolution mass spectra were obtained at the University of Texas at Austin Department of Chemistry and Biochemistry MS Facility. Elemental analyses were performed by Atlantic Microlabs Inc., Norcross, GA.

Preparation of [($C_{38}H_{32}N_8$)Cu^{II}_2] (3). One equivalent of the free base macrocycle, **1** (13.9 mg, 0.0230 mmol), was dried overnight in a Schlenk flask under vacuum. Next, the flask was charged with approximately 1 equiv of Cu_5Mes_5 (16.0 mg, 0.0222 mmol) and 20 mL of THF. Within 20 min the light yellow slurry became a dark brown solution. The reaction mixture was stirred overnight at ambient temperature before the solvent was removed under vacuum. The dark brown-green powder was redissolved in CH_2Cl_2, filtered, and exposed to air. Slow vapor diffusion of hexanes into CH_2Cl_2 produced 7.1 mg of **3** in the form of dark green crystals (45% yield). CI−HRMS M^+ *m*/*z* 727.14317 (calcd for $C_{38}H_{33}N_8Cu_2$ 727.14147). Anal. Calcd for $C_{38}H_{32}N_8Cu_2 \cdot 1/2CH_2Cl_2$: C, 60.03; H, 4.32; N, 14.55. Found: C, 60.09; H, 4.41; N, 14.31. This compound was also characterized by X-ray diffraction analysis (see below).

Preparation of [($C_{38}H_{36}N_8$)$Cu^{I}_2Cl_2$] (4). One equivalent of the free base macrocycle, **1** (90 mg, 0.149 mmol), was dissolved in 10 mL of CH_2Cl_2, and treated with 0.30 mL of 1 M HCl in diethyl ether, and stirred for 10 min at room temperature. After the solvent was removed the red-orange powder was dried overnight under vacuum. Then the flask was charged with approximately 1 equiv of Cu_5Mes_5 (100.0 mg, 0.1385 mmol) and 20 mL of THF. Within 30 min the red-orange slurry became an orange-brown solution. The solution was stirred overnight at ambient temperature and the solvent removed under vacuum. The brown-orange powder was redissolved in THF, filtered, and layered with *n*-pentanes to yield 36.7 mg of **4** as dark orange crystals (31% yield). ^{1}H NMR (400 MHz, CD_2Cl_2) δ 11.11 (br s, 4H, NH), 8.16 (s, 4H, imine CH), 7.27 (br d, 8H, aromatic CH), 6.83 (m, 4H, pyrrolic CH), 6.20 (m, 4H, pyrrolic CH), 2.22 (s, 6H, CH_3), 1.83 (s, 6H, CH_3). ^{13}C NMR (100 MHz, CD_2Cl_2) δ 148.8, 147.0, 145.0, 128.0, 127.4, 123.8, 117.7, 108.2, 36.8, 29.0, 27.0. Anal. Calcd for $C_{42}H_{40}N_8O_4Cu_2 \cdot$ 1.5THF: C, 58.02; H, 5.31; N, 12.30. Found: C, 58.64; H, 5.19; N, 12.37. This compound was also characterized by X-ray diffraction analysis (see below).

Preparation of [($C_{46}H_{52}N_8$)$Cu^{I}_2Cl_2$] (5). One equivalent of the free base macrocycle, **2** (41.2 mg, 0.0575 mmol), was dissolved in 10 mL of CH_2Cl_2, treated with 0.15 mL of 1 M HCl in diethyl ether and stirred for 20 min at room temperature. After removal of the solvent under reduced pressure, the red-orange powder was dried overnight. Next, the flask was charged with approximately 1 equiv of Cu_5Mes_5 (45.0 mg, 0.0623 mmol) and 20 mL of THF. The orange-brown solution was stirred overnight at ambient temperature before the solvent was removed under vacuum. The dark brown powder was redissolved in THF, filtered, and layered with *n*-pentanes to yield 29 mg of **5** as orange crystals (55% yield). ^{1}H NMR (400 MHz, CD_2Cl_2) δ 10.99 (br s, 4H, NH), 8.23 (s, 4H, imine CH), 7.24 (m, 8H, aromatic CH), 4.12 (s, 2H, CH_2), 4.08 (s, 2H, CH_2), 2.46 (q, 8H, CH_2CH_3), 2.23 (s, 12H, CH_3), 1.00 (t, 12H, CH_2CH_3). ^{13}C NMR (62 MHz, CD_2Cl_2) δ 146.0, 145.0, 134.5, 132.0, 127.0, 125.5, 125.0, 118.0, 17.5, 15.5, 9.5. Anal. Calcd for

(14) (a) Srinivasan, A.; Ishizuka, T.; Osuka, A.; Furuta, H. *J. Am. Chem. Soc.* **2003**, *125*, 878−879. (b) Tanaka, Y.; Hoshino, W.; Shimizu, S.; Youfu, K.; Aratani, N.; Maruyama, N.; Fujita, S.; Osuka, A. *J. Am. Chem. Soc.* **2004**, *126*, 3046−3407. (c) Shimizu, S.; Anand, V. G.; Taniguchi, R.; Furukawa, K.; Kato, T.; Yokoyama, T.; Osuka, A. *J. Am. Chem. Soc.* **2004**, *126*, 12280−12281.
(15) Li, R.; Mulder, T. A.; Beckmann, U.; Boyd, P. D. W.; Brooker, S. *Inorg. Chim. Acta* **2004**, *357*, 3360−3368.
(16) Arnold, P. L.; Blake, A. J.; Wilson, C.; Love, J. B. *Inorg. Chem.* **2004**, *43*, 8206−8208.
(17) Meyer, E. M.; Gambarotta, S.; Floriani, C.; Chiesi-Villa, A.; Guastini, C. *Organometallics* **1989**, *8*, 1067−1079.
(18) Sessler, J. L.; Cho, W.-S.; Dudek, S. P.; Hicks, L.; Lynch, V. M.; Huggins, M. T. *J. Porphyrin Phthalocyanine* **2003**, *7* (2), 97−104.

Table 1. Crystal Data and Structure Refinement Parameters for **3** and **5**

	3	**4**	**5**
empirical formula	$C_{39.5}H_{35}Cl_3Cu_2N_8 \cdot 3/2CH_2Cl_2$	$C_{46}H_{52}Cl_2Cu_2N_8O_2 \cdot 2C_4H_8O$	$C_{58}H_{64}Cl_2Cu_{2\ 8}O_3 \cdot 3C_4H_8O$
fw	855.18	946.94	1119.18
cryst syst	orthorhombic	monoclinic	monoclinic
space group	*Pbca*	*P*21/*n*	*C*2/*c*
a, Å	14.7258(2)	16.9594(1)	24.2390(6)
b, Å	20.3270(2)	15.0893(1)	15.9732(4)
c, Å	25.0991(3)	18.9670(2)	14.2036(4)
α, deg	90	90	90
β, deg	90	114.5110(5)	98.937(1)
γ, deg	90	90	90
V, Å^3	7512.9(1)	4416.34(6)	5432.5(2)
Z	8	4	4
D (calcd), mg/m^3	1.512	1.424	1.381
abs coeff, mm^{-1}	1.387	1.132	0.934
F(000)	3496	1968	2376
cryst size	0.37 × 0.12 × 0.09	0.30 × 0.26 × 0.25	0.61 × 0.08 × 0.06
q for data collection	2.93−27.48	2.95−27.49	2.93−27.43
limiting indices	$-15 \le h \le 19$	$-21 \le h \le 22$	$-29 \le h \le 30$
	$-26 \le k \le 26$	$-19 \le k \le 19$	$-20 \le k \le 20$
	$-32 \le l \le 32$	$-24 \le l \le 24$	$-18 \le l \le 18$
reflns collected	70 825	19 669	11 259
independent reflns	8594	10 107	6112
completeness to *θ*	99.9%	99.8%	98.5%
abs corr	Gaussian	none	none
data/restraints/params	8594/18/487	10107/12/568	6112/2/272
goodness-of-fit on F^2 [a]	1.068	1.142	1.415
R, R_w [b]	0.0544, 0.1337	0.0456, 0.1222	0.0567, 0.1220

[a] Goodness of fit, *S*, $[\sum w(|F_o|^2 - |F_c|^2)^2/(n-p)]^{1/2}$. [b] $R = \sum(|F_o| - |F_c|)/\sum|F_o|\}$ for reflections with $F_o > 4(\sum(F_o))$. $R_w = \{\sum w(|F_o|^2 - |F_c|^2)^2/\sum w(|F_o|)^4\}^{1/2}$.

$C_{46}H_{52}N_8Cu_2Cl_2 \cdot 4CH_2Cl_2$: C, 47.86; H, 4.82; N, 8.93. Found: C, 47.96; H, 4.91; N, 9.01. This compound was also characterized by X-ray diffraction analysis (see below).

X-ray Diffraction Analysis. The data were collected on a Nonius Kappa CCD diffractometer using a graphite monochromator with Mo Kα radiation ($\lambda = 0.710\,73$ Å). The data were collected at 153 K using an Oxford Cryostream low-temperature device. Data reduction were performed using DENZO-SMN.[19] The structure was solved by direct methods using SIR97[20] and refined by full-matrix least-squares on F^2 with anisotropic displacement parameters for the non-H atoms using SHELXL-97.[21] All hydrogen atoms were calculated in ideal positions with isotropic displacement parameters set to 1.2Ueq of the attached atom (1.5Ueq for methyl hydrogen atoms).

X-ray Experimental for 3, $[(C_{38}H_{32}N_8)Cu_2]\cdot 3/2CH_2Cl_2$. Crystals grew as dark green almost black needles by vapor diffusion of hexanes into a methylene chloride solution of the copper complex. A total of 335 frames of data were collected using *ω* scans with a scan range of 1° and a counting time of 203 s per frame. Details of crystal data, data collection, and structure refinement are listed in Table 1.

X-ray Experimental for 4, $[(C_{38}H_{36}N_8)Cu_2Cl_2]\cdot 2C_4H_8O$. Crystals grew as orange-brown prisms by diffusion of *n*-pentane into a THF solution of the macrocyclic complex. A total of 461 frames of data were collected using *ω* scans with a scan range of 1° and a counting time of 111 s per frame. Details of crystal data, data collection, and structure refinement are listed in Table 1.

Two large peaks persisted in the electron density map after all the expected atoms were accounted for. The largest peak was near Cu2 and within bonding distance of the imine nitrogen atoms, N6 and N7, and the chloride ion, Cl2. It was assumed that this peak was due to an occupational disorder of Cu2, which had a slightly higher Ueq than did Cu1. The site occupancy factor for this pair of atoms was refined by assigning the variable *x* to the site occupancy for Cu2 and $(1 - x)$ to the site occupancy for Cu2a. At the same time as the site occupancy factor was refined, a common isotropic displacement factor was refined for both Cu2 and Cu2a. In this way, the site occupancy for Cu2 refined to 92(2)%. In addition, a smaller peak persisted in the difference electron density map and was found to be 1.87 Å from pyrrole nitrogen atom, N5. This peak could not be explained in a chemically reasonable way and was not accounted for in the final refinement model. Both the peak near Cu2 and the unexplained peak near N5 persisted in two data collections on two different batches of crystals.

The function $\Sigma w(|F_o|^2 - |F_c|^2)^2$ was minimized, where $w = 1/[(\sigma(F_o))^2 + (0.0493P)^2 + (2.5494P)]$ and $P = (|F_o|^2 + 2|F_c|^2)/3$. $R_w(F^2)$ refined to 0.122, with $R(F)$ equal to 0.0456 and a goodness of fit, *S*, of 1.14.[22] The data were checked for secondary extinction effects, but no correction was necessary. Neutral atom scattering factors and values used to calculate the linear absorption coefficient are from the International Tables for X-ray Crystallography.[23]

X-ray Experimental for 5, $[(C_{46}H_{52}N_8)Cu_2Cl]\cdot 3C_4H_4O$. Crystals grew as orange-brown needles by diffusion of *n*-pentane into a THF solution of the macrocyclic complex. A total of 342 frames of data were collected using *ω* scans with a scan range of 1° and a counting time of 170 s per frame. Details of crystal data, data collection, and structure refinement are listed in Table 1.

The macrocyclic Cu complex resides on a crystallographic 2-fold rotation axis at 0, *y*, 3/4. The chloride ions lie on the 2-fold rotation

(19) Otwinowski Z.; Minor W. In *Methods in Enzymology*; Carter, J., Sweets, R. M., Eds.; Academic Press: New York, 1997; Vol. 276, pp 307−326, C.

(20) Altomare, A.; Burla, M. C.; Camalli, M.; Cascarano, G. L.; Giacovazzo, C.; Guagliardi, A.; Moliterni, A. G. G.; Polidori, G.; Spagna, R. *J. Appl. Crystallogr*. **1999**, *32*, 115−119.

(21) Sheldrick, G. M. *SHELXL97*; *Program for the Refinement of Crystal Structures*; University of Gottingen: Gottingen, Germany, 1994.

(22) $R_w(F^2) = \{\Sigma w(|F_o|^2 - |F_c|^2)^2/\Sigma w(|F_o|)^4\}^{1/2}$, where *w* is the weight given each reflection. $R(F) = \Sigma(|F_o| - |F_c|)/\Sigma|F_o|\}$ for reflections with $F_o > 4(\sigma(F_o))$. $S = [\Sigma w(|F_o|^2 - |F_c|^2)^2/(n-p)]^{1/2}$, where *n* is the number of reflections and *p* is the number of refined parameters.

(23) *International Tables for X-ray Crystallography*; Wilson, A. J. C., Ed.; Kluwer Academic Press: Boston, 1992; Vol. C, Tables 4.2.6.8 and 6.1.1.4.

Scheme 1

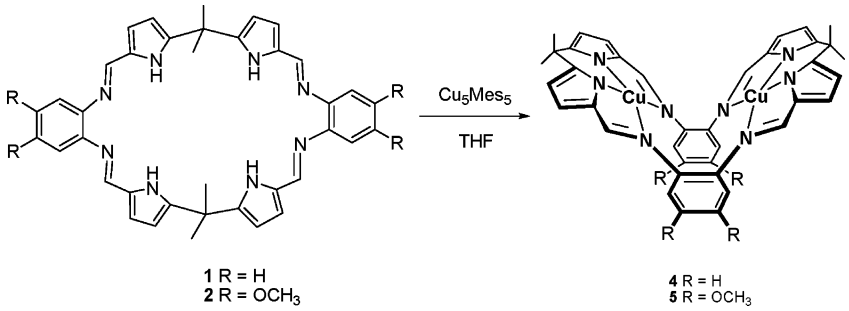

axis, which bisects the macrocycle. In addition to the Cu complex, there are two regions of disordered solvent. The solvent appears to be THF. One of the solvate molecules lies near the 2-fold rotation axis, while the other lies on a general position. The contribution to the scattering due to the disordered solvent was removed by use of the utility SQUEEZE in PLATON98 as incorporated in WinGX.[24] The methyl carbon bound to C18 was found to be disordered about two orientations. The site occupancy of the two orientations were refined while refining a common isotropic displacement parameter for the two atoms, C19 and C19a. The site occupancy factor refined to a value very close to 1/2 and was subsequently fixed at 1/2.

Magnetic Measurements. The solid-state magnetic susceptibility of a crystalline sample of **3** was measured between 4 and 300 K at a field of 1 kOe using a Quantum Design Model MPMS SQUID magnetometer. The sample was placed in a gelatin capsule. The susceptibility of the capsule was measured and its contribution subtracted from the overall susceptibility (for more details see Supporting Information).

The room-temperature solution magnetic moment of **3** was measured using the Evans[25] method. A solution of the metal complex was prepared in $CDCl_3$ and placed in a 5 mm NMR tube, while pure $CDCl_3$ was placed in a concentric capillary tube within the NMR tube. The calculation of the magnetic moment (μ) was based on the difference in chemical shift observed for the residual $CHCl_3$ signal in neat solvent and in the solution containing the paramagnetic species (for more details see Supporting Information).

Results and Discussion

Synthesis and Characterization of Bimetallic Copper Complexes. In our previous study of ligands analogous to **1** and **2** we used iron(II) mesitylene as the metal cation source.[3] Subsequent oxidation then provided the corresponding iron(III) complexes, with the specific structure of these final products being found to depend on the protonation state of the starting, metal-free ligand. The success of this work led us to consider a study of the analogous copper chemistry. Both Cu(I) and Cu(II) were expected to be stabilized by the same, or nearly the same, macrocyclic ligand, albeit the coordination geometry around each metal center should change with the oxidation state of the copper atoms (i.e., putative Cu(I) complexes were expected to be characterized by tetrahedral geometries, while square planar geometries would be expected for the Cu(II) complexes). Again, in exploring this chemistry the use of a mesitylene reagent, in this case Cu_5Mes_5, proved appealing; it would provide a readily available source of metal ion and a built-in deprotonating agent, meaning that, unless desired, no additional anionic counterion would need to be added to the reaction mixture.

In terms of specifics, the bimetallic Cu(II) complex of ligand **1** (complex **3**; Scheme 1) was prepared by combining 1 equiv of the corresponding free base macrocycle with excess copper(I) mesitylene in THF at room temperature under argon. The resulting dark brown solution, presumably containing one or more coordinated Cu(I) species, was stirred overnight at room temperature. Subsequent air oxidation then gave the bis-copper(II) complex **3** as dark green crystals in 45% yield after subjecting the crude product to recrystallization (slow diffusion of hexanes into a methylene chloride solution). Elemental analysis, mass spectrometry, and X-ray crystallography (see below) proved consistent with the proposed bis-copper(II) adduct.

Unfortunately, as yet, we have been unable to characterize any well-defined Cu(I) species from the initial reaction mixture leading to complex **3**. However, as noted above, in our previous work with iron mesitylene we found that the protonation state of macrocycles **1** and **2** had a profound influence on the coordination environment of the iron centers in the isolated μ-oxo Fe(III) dimers.[3] Thus, we also examined the metalation chemistry of the bis HCl salts of macrocycles **1** and **2**. The relevant chemistry is summarized in Schemes 2 and 3. In a typical reaction, 2 equiv of HCl were added to 1 equiv of the free base macrocycle in CH_2Cl_2 to form what was presumed to be the bis-HCl salt of the ligand as a red-orange solution. Next, the solvent was removed and the flask charged with 1 equiv of Cu_5Mes_5 and 20 mL of dry oxygen-free THF to give a yellow-brown solution that was stirred overnight at room temperature. After removal of the solvent, the brown powder was redissolved in THF and layered with *n*-pentane to give air-sensitive yellow-brown crystals of the resulting bimetallic Cu(I) complex, **4** or **5**, in 30−55% yield. Complexes **4** and **5** were characterized by elemental analysis, ^{1}H and ^{13}C NMR spectroscopy, and X-ray crystallography (see below).

The room-temperature ^{1}H NMR spectrum of **4** contains seven unique proton resonances, and that of **5** contains eight unique proton resonances. Both spectra are consistent with the structures proposed in Schemes 2 and 3 and reveal that in solution complexes **4** and **5** are highly symmetric. The

(24) Squeeze-Platon98-WingX: (a) Spek, A. L. *PLATON, A Multipurpose Crystallographic Tool*; Utrecht University: Utrecht, The Netherlands, 1998. (b) Farrugia, L. J. *J. Appl. Crystallogr.* **1999**, *32*, 837−838.

(25) (a) Evans, D. F. *J. Chem. Soc.* **1959**, 2003−2005. (b) Grant, D. H. *J. Chem. Educ.* **1995**, *72*, 39−40. (c) Schubert, E. M. *J. Chem. Educ.* **1992**, *69*, 62.

Scheme 2

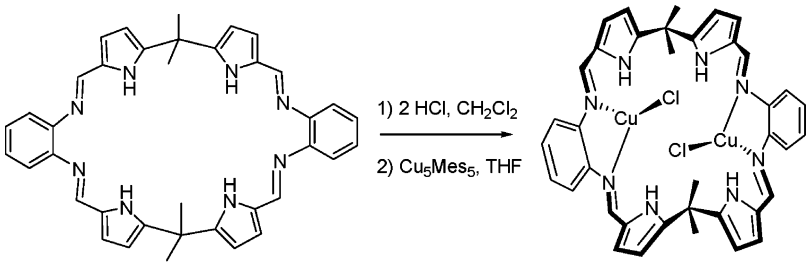

1 6

Scheme 3

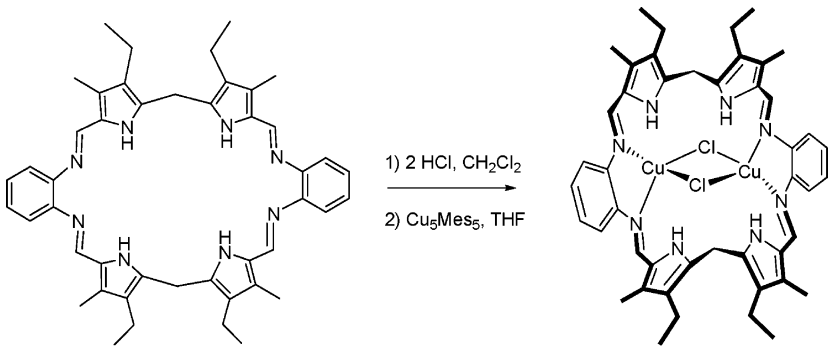

3 7

^{1}H NMR spectra also confirm that each of the four pyrrolic nitrogen atoms in **4** and **5** are protonated (i.e., $\delta = 11.11$ and 10.99 for **4** and **5**, respectively, each integrating to four protons).

Once characterized, complexes **4** and **5** were dissolved in CH_2Cl_2 and exposed to air. Mass spectrometric analyses of the resulting solutions confirmed that the copper atoms present in **4** and **5** remained coordinated to the macrocycles after air oxidation. However, it is interesting to note that crystals isolated from the oxidation reaction of **4** were characterized by elemental analysis and X-ray diffraction and found to correspond to a complex similar to **3** (see the Supporting Information for the crystallographic data of this bis-Cu(II) complex, **3′**). Despite some minor differences (possibly due to different crystallization conditions), the complex obtained from air oxidation of **4** contains exactly the same connectivity found in complex **3**. In complex **4** the macrocycle supports the coordination of two Cu(I) cations by acting as a bis-bidentate ligand through the two phenylene diimine units. However, upon air oxidation the macrocycle becomes a bis-tetradentate ligand and coordinates each Cu(II) cation through the pyrrole nitrogen atoms of a dipyrromethane unit and one imine nitrogen atom from each phenylenediimine unit. This dramatic change in the coordination mode upon oxidation of the coordinated cations from Cu(I) to Cu(II) parallels what was seen recently in the case of a rather different bipyrrole-type Schiff base macrocycle[1] and serves to highlight further the versatility of the present dipyrromethane-derived Schiff base ligands.

Crystallographic Characterization of 3−5. Single-crystal X-ray diffraction analysis was performed on crystals of **3**−**5**, and the resulting structures are shown in Figures 2−4, with selected bond lengths and angles listed in Tables 2 and 3. These figures reveal that in each complex the macrocycle is coordinated to two copper atoms. However, the nature of the binding mode differs as a function of oxidation state of the metal cation (**3** vs **4**) and ligand type (**4** vs **5**).

The crystal structure for complex **3** is reminiscent of the bis-Cu(II) accordion porphyrin originally reported by Mertes and co-workers (Figure 5, complexes **6**)[4,5] and other dipyr-

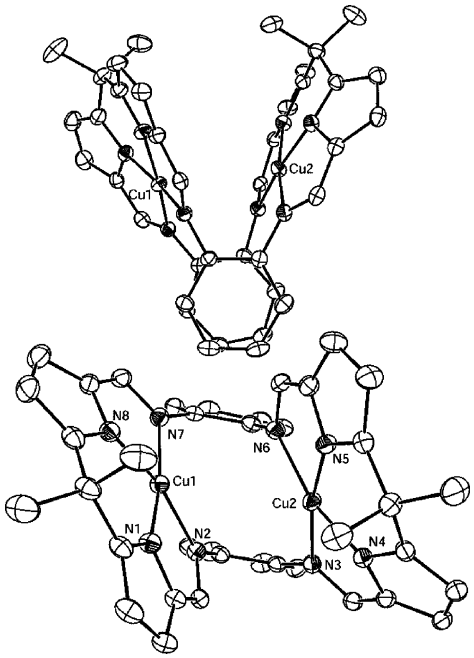

Figure 2. Two views of **3** showing partial atom-labeling schemes. Displacement ellipsoids are scaled to the 35% probability level. The hydrogen atoms have been removed for clarity. The lattice contains 1.5 molecules of CH_2Cl_2, not shown.

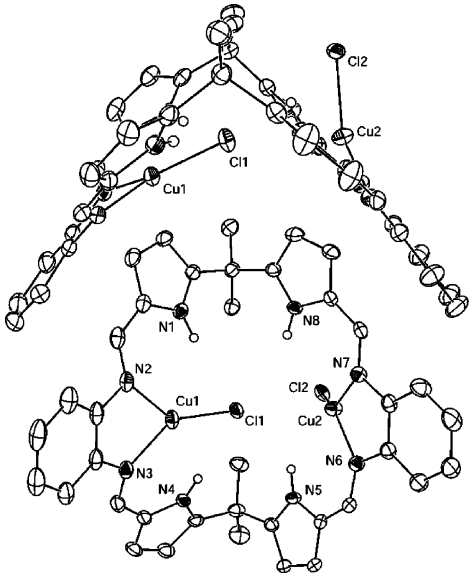

Figure 3. Two views of **4** showing partial atom-labeling schemes. Displacement ellipsoids are scaled to the 35% probability level. Most hydrogen atoms and two THF solvent molecules have been removed for clarity. The disorder for Cu2 is not shown (see Experimental Section for details).

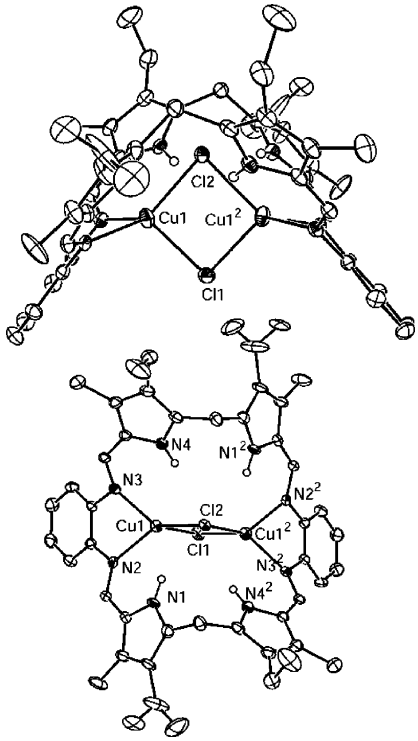

Figure 4. Two views of **5** showing partial atom-labeling schemes. Displacement ellipsoids are scaled to the 35% probability level. The macrocyclic Cu complex resides on a crystallographic 2-fold rotation axis at 0, *y*, 3/4. The chloride ions lie on the 2-fold rotation axis which bisects the macrocycle. Most hydrogen atoms and two regions of disordered solvent have been removed for clarity.

romethane Schiff base macrocycles recently described by Brooker and co-workers (Figure 5, complexes **7**).[6] The geometry around each metal center in **3** is square planar (the sum of the N−Cu−N angles around is 358.92° for Cu1 and 359.14° for Cu2 and the largest deviation from the mean plane is 0.078(2) Å for Cu1 and 0.128(2) for Cu2). Each

Table 2. Selected Bond Lengths (Å) and Angles (deg) for **3**

Cu1−N1	1.897(3)	N2−Cu1−N7	108.69(13)
Cu1−N2	2.040(3)	N7−Cu1−N8	82.07(14)
Cu1−N7	1.996(3)	N8−Cu1−N1	86.57(14)
Cu1−N8	1.903(3)	N1−Cu1−N2	82.59(13)
Cu2−N3	1.994(3)	N7−Cu1−N1	168.64(14)
Cu2−N4	1.925(3)	N8−Cu1−N2	166.25(14)
Cu2−N5	1.909(3)	N3−Cu2−N4	81.73(14)
Cu2−N6	2.069(3)	N4−Cu2−N5	87.43(14)
Cu1···Cu2	3.473(3)	N5−Cu2−N6	81.97(13)
		N6−Cu2−N3	108.01(13)
		N3−Cu2−N5	168.46(13)
		N6−Cu2−N4	165.74(14)

Table 3. Selected Bond Lengths (Å) and Angles (deg) for **4** and **5**

	4	**5**
Cu1−N2	2.000(2)	2.084(3)
Cu1−N3	2.013(2)	2.059(3)
Cu1···N1	3.273	3.280
Cu1···N4	3.271	3.305
Cu1−Cl1	2.1395(7)	2.333(1)
Cu1−Cl2		2.412(1)
Cu2−N6	2.024(2)	*a*
Cu2−N7	2.024(2)	*a*
Cu1···N1	3.273	3.280
Cu1···N4	3.271	3.305
Cu2···N5	3.215	*a*
Cu2···N8	3.285	*a*
Cu2···N5	3.215	*a*
Cu2···N8	3.285	*a*
Cu2−Cl1		*a*
Cu2−Cl2	2.1855(8)	*a*
Cu1···Cu2	4.987	3.290
Cu1−Cl1−Cu2		89.68(5)
Cu1−Cl2−Cu2		85.99(5)
Cl2−Cu1−Cl1		92.16(3)
N2−Cu1−N3	84.80(10)	81.03(11)
N6−Cu2−N7	83.89(10)	*a*
N2−Cu1−Cl2	137.08(8)	109.43(8)
N2−Cu1−Cl2		129.95(8)
N3−Cu1−Cl1	138.08(8)	118.88(8)
N3−Cu1−Cl2		127.42(9)
N6−Cu2−Cl1		*a*
N6−Cu2−Cl2	135.14(7)	*a*
N7−Cu2−Cl1		*a*
N7−Cu2−Cl2	134.70(7)	*a*

[a] Complex **5** lies on a crystallographic mirror plane of symmetry that bisects the complex.

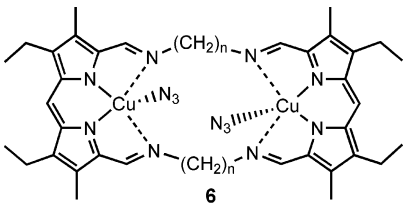

6

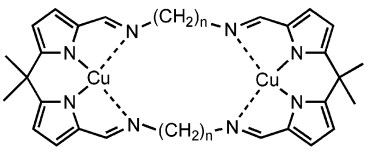

7

Figure 5. Chemdraw representations of previously reported bis-Cu(II) complexes **6** and **7** (see refs 4 and 6).

Cu(II) center is bound to one of the pyrrole nitrogen atoms from each of the two dipyrromethane units and to one of the imine nitrogen atoms from each of the phenylenediimine units. The individual N−Cu−N bond angles for **3** are

between 81.73° and 108.69°, with the largest angles being formed between a copper atom and two imine nitrogen atoms and the smallest angles occurring between a copper atom and two pyrrole nitrogen atoms. These angles compare well with those previously reported for bimetallic Cu(II) dipyrromethane Schiff base macrocycles (N−Cu−N bond angles of 79.3−110.7°).[4−6] The $Cu-N_{pyrrole}$ distances for **3** (1.897−1.925 Å) are slightly shorter than the $Cu-N_{imine}$ (1.996−2.069 Å) distances. Both distances are comparable to the ones seen in the Schiff base complexes reported by Mertes (complex **6**; $Cu-N_{pyrrole}$ 1.914−1.999 Å and $Cu-N_{imine}$ 2.034−2.150 Å)[4] and Brooker (complex **7**; $Cu-N_{pyrrole}$ 1.881−1.934 Å and $Cu-N_{imine}$ 1.986−2.068 Å).[6] However, complex **3** differs significantly from the previously characterized bimetallic Cu(II) Schiff base dipyrromethane macrocycles with regard to the distance between the two Cu(II) metal centers. In complex **3** the Cu1−Cu2 distance is 3.473(3) Å, while the corresponding inter-copper distance is 5.393(2) Å in the Mertes system (Figure 5, complex **6**, $n = 3$). Both sets of distances are shorter than those reported by Brooker for her somewhat analogous systems, namely, 6.5063(19) and 8.3235(12) Å, respectively, for the separation between the two Cu(II) metal centers in complexes **7**, $n = 3$ and 4, of Figure 5.

The structures for complexes **4** and **5**, shown in Figures 3 and 4, respectively, correspond to the bimetallic Cu(I) complexes that form from the reactions shown in Schemes 2 and 3. These structures make it clear that the presence of HCl during the synthesis of **4** and **5** has a strong effect on the binding mode of the copper. In both structures each copper atom is bound to two nitrogen atoms from a single phenylenedimine unit and to at least one chlorine atom. However, the X-ray structure for complex **4** contains significant disorder around one of the Cu atoms, and although this disorder has been modeled (see experimental), a definitive characterization of the structure for **4** cannot be made at this time. Thus, the quantitative discussion of the metal geometries will be limited to complex **5**. Complex **5** contains a crystallographic 2-fold rotation axis at 0, *y*, 3/4 and two bridging Cl atoms. The geometry around each metal center is a distorted tetrahedron (the angle between the N3−N2−Cu1 plane and the Cl1−Cl2−Cu1 plane is 96.3(1)°) with a N−Cu−N angle of 81.03(11)°, a Cl−Cu−Cl angle of 92.16(3)°, and N−Cu−Cl angles of 129.95(8)° and 118.88(8)°. The $Cu-N_{imine}$ distances for **5** are 2.084(3) and 2.059(3) Å, and the Cu−Cl distances are 2.333(1) and 2.412(1) Å (the Cu−Cl distances compare well with those in similar complexes reported by our group, 2.366-2.476 Å[7d]). Finally, the flexibility of the macrocycle allows the ligand to fold and bring the two Cu(I) metal centers close together, resulting in a Cu−Cu distance of 3.290 Å, which is shorter than that seen in complex **3** (3.473(3) Å) as well as in the bis-Cu(I) complex of the bipyrrole Schiff base macrocycle recently reported by our group (Cu−Cu, 5.296 Å).[1,26]

(26) A shorter Cu−Cu distance has however been observed in a hexapyrrolic non-Schiff base expanded porphyrin complex (Cu−Cu, 2.761(1) Å; see ref 7d).

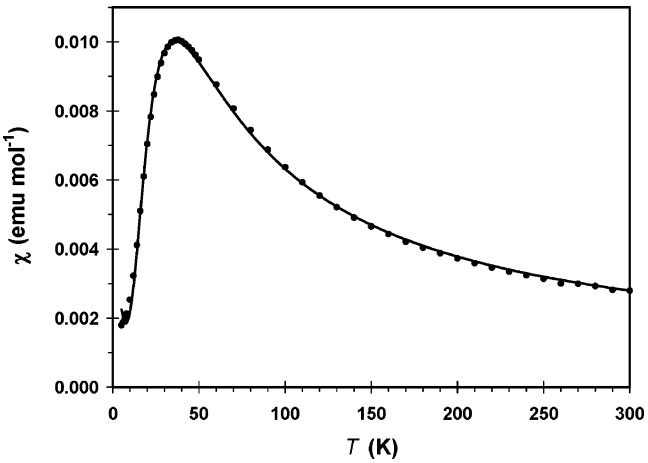

Figure 6. SQUID data for **3** (plot of χ vs T). The line shown is the theoretical fit to a modified Bleaney−Bowers equation (see Supporting Information for complete details).

Magnetic Suceptibility. The relatively short Cu−Cu distance (3.473 Å) found in the X-ray crystal structure of **3** led us to examine the magnetic properties of this complex. First, we determined the room-temperature, spin-only magnetic moment (μ_{eff}) of complex **3** in deuterated chloroform using the Evans method.[25] Measurements were performed at two different concentrations to give values of $\mu_{eff} = (2.0 \pm 0.1)\ \mu_B$ for **3**. These values are lower than the expected magnetic moment ($\mu_{eff} = 2.45\ \mu_B$) for two isolated Cu(II) metal centers ($S = 1/2$). To investigate the magnetism of this complex further, SQUID magnetometry was used to measure the solid-state magnetic susceptibility, χ, for **3** over a temperature range of 4−300 K in a 1 kOe field. The results of this study are shown in Figure 6. As the temperature is lowered, χ increases until a maximum is reached at approximately 38 K, indicating an antiferromagnetic interaction between Cu(II) metal centers. The data were fit to a modified Bleaney−Bowers equation (see Supporting Information for more details). The fit of the data resulted in a J value of $-41.0 \pm 0.2\ cm^{-1}$, indicative of weak antiferromagnetic coupling between metal centers in **3**. The small $-J$ value observed for **3** is as predicted given the absence of a Cu−Cu bond or a direct single-atom bridge between the Cu(II) metal centers in **3**. (Note: In **3** the only connection between the Cu(II) metal centers is via a four-atom π-conjugated bridge). A similar observation has been made by Brooker et al. for bimetallic Cu(II) complexes of pyridazine-linked Schiff base macrocycles.[27]

Conclusions

We have prepared and fully characterized a new bimetallic Cu(II) complex, **3**, of the expanded porphyrin Schiff base macrocycle, **1**, and have shown that Cu(I) derivatives of this ligand can be prepared when the macrocycle is fully protonated before metalation. Two new Cu(I) complexes, **4**

(27) Brooker et al. report $J = -13.2\ cm^{-1}$ for a bimetallic Cu(II) complex of a Schiff base macrocycle wherein the Cu(II) metal centers are connected by five-atom (Cu−N−N−C−C−N−Cu) pyridazine-linked bridges and the distance between the two Cu(II) metal centers is 5.874(2) Å, see: Brooker, S.; Ewing, J. D.; Ronson, T. K.; Harding, C. J.; Nelson, J.; Speed, D. J. *Inorg. Chem.* **2003**, *42*, 2764−2773.

and **5**, have been isolated and characterized by X-ray crystallography. This structural analysis provides support for the notion that in addition to any inherent geometric preference displayed by the coordinated cation (d^{10} Cu(I) vs d^9 Cu(II)), the choice of starting ligand (substitution pattern, protonation, and presence of counterions) has a strong influence on the binding mode of the coordinated metal centers in these complexes. The Cu−Cu distance in complex **3** (3.473 Å) was found to be relatively short as compared to what is seen in similar oligopyrrole-derived Schiff base complexes. The room-temperature magnetic moment for **3**, $\mu_{\text{eff}} = (2.0 \pm 0.1)\ \mu_B$, was found to be slightly below the expected value for two noninteracting Cu(II) spins ($2.45\ \mu_B$), while variable-temperature SQUID data for **3** was consistent with the two Cu(II) metal centers being weakly antiferromagnetically coupled ($J = -41.0 \pm 0.2\ \text{cm}^{-1}$). These results, together with those reported previously,[1] demonstrate that oligopyrrolic Schiff base macrocycles are flexible and versatile ligands capable of stabilizing complexes with metals in different oxidation states and different coordination environments. These attributes could make such systems attractive as ligands for the development of new kinds of metalloenzyme mimics.

Acknowledgment. This work was supported by the National Institutes of Health (Grant No. CA 68682 to J.L.S. and Grant No. GM20834-02 to J.M.V.) and by the Robert A. Welch Foundation (Grant Nos. F-1191 and F-1018 to J.T.M. and J.L.S., respectively). The authors thank Luca Olivi and R. Jason Scharff for helpful discussions.

Supporting Information Available: CIFs for **3**−**5** and magnetic susceptibility data for **3**. This material is available free of charge via the Internet at http://pubs.acs.org.

IC050690D